Colloids and Surfaces B: Biointerfaces 88 (2011) 559–567

Contents lists available at ScienceDirect

Colloids and Surfaces B: Biointerfaces

journal homepage: www.elsevier.com/locate/colsurfb

# Influence of boundary on the effect of double-layer polarization and the electrophoretic behavior of soft biocolloids

Li-Hsien Yeh [a], Kuo-Ying Fang [a], Jyh-Ping Hsu [a,*], Shiojenn Tseng [b]

[a] Department of Chemical Engineering, National Taiwan University, Taipei 10617, Taiwan
[b] Department of Mathematics, Tamkang University, Tamsui, Taipei 25137, Taiwan

ARTICLE INFO

*Article history:*
Received 12 May 2011
Received in revised form 10 July 2011
Accepted 15 July 2011
Available online 23 July 2011

*Keywords:*
Electrophoresis
Biocolloids
Soft particles
Boundary effect
Double-layer polarization
Electroosmotic retardation flow

ABSTRACT

The electrophoresis of a soft particle comprising a rigid core and a charged porous membrane layer in a narrow space is modeled. This simulates, for example, the capillary electrophoresis of biocolloids such as cells and microorganisms, and biosensor types of device. We show that, in addition to the boundary effect, the effects of double-layer polarization (DLP) and the electroosmotic retardation flow can be significant, yielding interesting electrophoretic behaviors. For example, if the friction coefficient of the membrane layer and/or the boundary is large, then the DLP effect can be offset by the electroosmotic retardation flow, making the particle mobility to decrease with increasing double layer thickness, which is qualitatively consistent with many experimental observations in the literature, but has not been explained clearly in previous analyses. In addition, depending upon the thickness of double layer, the friction of the membrane layer of a particle can either retard or accelerate its movement, an interesting result which has not been reported previously. This work is the first attempt to show solid evidence for the influence of a boundary on the effect of DLP and the electrophoretic behavior of soft particles. The model proposed is verified by the experimental data in the literature. The results of numerical simulation provide valuable information for the design of bio-analytical apparatus such as nanopore-based sensing applications and for the interpretation of relevant experimental data.



## 1. Introduction

Electrophoresis has been applied widely in many areas of fundamental and practical significance. Recent advances in fabrication techniques further extend its application to small-scaled operations such as capillary electrophoresis [1,2], lab-on-a-chip devices [3,4], biosensors [5], and nanopore sensing technology [6–8]. In these cases, because the available space for electrophoresis is narrow, the electrophoretic behavior of a particle is influenced inevitably by the boundary of a device. This effect is usually ignored in the early stage of electrophoresis analysis. In fact, the presence of a boundary can have a profound influence on that behavior. For example, if a particle is sufficiently close to a surface, then its electrophoretic velocity can be either raised or reduced, depending upon the neighboring conditions [9–11]. It is also possible that the direction of electrophoresis is altered by a nearby surface [12,13].

Conventional electrophoresis analysis focused mainly on a rigid particle, where its surface is impenetrable to ionic species and fluid medium. Recently, a more general type of particle, namely, soft or fuzzy particle, is proposed to simulate biocolloids such as cells and microorganisms and inorganic particles covered by an artificial membrane layer [14–18]. A soft particle comprises a rigid core and a porous layer, which is penetrable to ionic species and fluid medium. Note that a rigid particle can be viewed as the limiting case of a soft particle where its porous layer is infinitely thin. On the other hand, if the rigid core of a soft particle is infinitely small, then it becomes entirely porous. Polyelectrolytes such as DNA, proteins, and polymer gels, for instance, belong to this category [19,20]. In addition to the charge on the surface of its rigid core, the porous layer of a soft particle is also capable of carrying charge, which comes from, for example, the dissociation/association reactions of function groups. This implies that the electrophoretic behavior of a soft particle can be more complicated than that of the corresponding rigid particle.

Several attempts have been made recently on the modeling of the electrophoresis of soft particles. Ohshima [21–27], for example, conducted a series of theoretical studies on the electrophoretic behaviors of soft particles under the conditions of weak applied electric field and low surface potential. The latter assumption implies that the effect of double-layer polarization (DLP), one of the interesting phenomena in electrophoresis coming from the deformation of double layer when the particle is in motion [28], can be neglected. Under the same conditions, Zhang et al. [29] and Hsu et al. [30,31] investigated further the boundary effect on the electrophoretic behavior of a soft particle by considering the elec-

* Corresponding author. Tel.: +886 2 23637448; fax: +886 2 23623040.
*E-mail address:* jphsu@ntu.edu.tw (J.-P. Hsu).

0927-7765/$ – see front matter © 2011 Elsevier B.V. All rights reserved.
doi:10.1016/j.colsurfb.2011.07.033

trophoresis of a soft toroid [30] and a sphere [29,31] along the axis of a cylindrical pore. Yeh et al. [32] analyzed the electrophoresis of a membrane-coated cylinder positioned eccentrically along the axis of a cylindrical pore for the case of arbitrary double-layer thickness, which is a three-dimensional problem. Taking the effect of DLP, which usually retards the particle motion, into account, Saville [33] and Hill et al. [34] studied the electrophoresis of an isolated soft spherical particle in an unbounded electrolyte solution. It was found that the effect of DLP can be significant when the charge density of a soft particle is high. Those analyses were extended by Lee et al. [35] to take the effect of particle concentration into account. The influence of a boundary on the electrophoretic behavior of a soft sphere for the case of an arbitrary level of surface potential, where applying a nonlinear Poisson–Boltzmann equation to describe the electrical potential is necessary, was analyzed by several investigators through considering various geometries [36–38].

Two types of soft particle have been considered in previous theoretical studies. For convenience, we define type I soft particle as the one with a charged rigid core having a constant surface potential and an ion-penetrable porous layer [25–27,31–38], and type II soft particle as the one with an uncharged rigid core and a polyelectrolyte membrane layer [21–24,29,30]. Note that a Neumann type of boundary condition, imposing a zero charge density on the surface of the rigid core of a particle, is applied in case of type II soft particle. Therefore, the electrical potential on that surface, known as Donnan potential [17,21], varies with the physicochemical properties of the membrane layer of the particle and the electrolyte concentration. This model predicts that the electrophoretic mobility of a particle decreases with decreasing double layer thickness [24]. This is consistent with the behavior of biocolloids such as cells, proteins, microorganisms, and inorganic particle covered by a biological membrane layer [18,20,39,40]. On the other hand, a Dirichlet type of boundary condition, imposing a constant potential on the surface of the rigid core of a particle, is applied in the case of type I soft particle. In this case, the electrophoretic mobility of a particle increases with decreasing double layer thickness, in general [25–27,31–38]. This phenomenon is similar to that of a rigid particle having a constant surface potential [9–13].

Taking the effect of DLP into account, the influence of a boundary on the electrophoretic behavior of a soft biocolloid (type II soft particle) is investigated in this study by considering the electrophoresis of a soft sphere in a spherical cavity. This geometry was adopted by Zydney [41] to simulate the electrophoresis of a rigid sphere in a porous medium, and by others to model that of a concentrated dispersion [42,43]. As pointed out by Lee et al. [44], although the sphere-in-spherical cavity model is an idealized one, it is relatively simple in mathematical representation and can be used to predict the behavior of a sphere in a cylindrical pore. The electrophoretic mobility of the particle under various conditions is examined in detail through varying the thickness of double layer, the position of the particle in the cavity, the properties of the membrane layer of the particle, and the size of the cavity. Since the position of the particle is arbitrary, the geometry considered is capable of simulating more realistically the experiments in practice, such as the characterization of biocolloids by capillary electrophoresis [18,39,40] and the electrophoretic translocation of protein [45,46] and DNA [6–8], through a nanopore. This study is also aimed to provide theoretical background for the interpretation of the dependence of the electrophoretic mobility of biocolloids on salt concentration usually observed in experiments.

## 2. Theory

The problem under consideration is illustrated in Fig. S1 of Supplementary Material, where a soft sphere of radius $a$ comprising a rigid core of radius $(a–c)$ and an ion-penetrable membrane layer of thickness $c$ at an arbitrary position in a spherical cavity of radius $b$ is driven by an applied uniform electric field $\mathbf{E}$ of strength $E$ in the $z$-direction. The cylindrical coordinate $(r,\theta,z)$ is adopted with the origin located at the center of the cavity, and the center of the particle is at $z = m$. Let $\Lambda = a/b$ and $M = 100\% \times [m/(b-a)]$ be the relative size of the cavity and the relative position of the particle, respectively. Note that the larger the $\Lambda$ or $M$ the more important the boundary effect is. The cavity is filled with an aqueous, incompressible Newtonian fluid containing $z_1{:}z_2$ electrolytes with $z_1$ and $z_2$ being the valences of cations and of anions, respectively.

If we let $\phi$, $n_j$, $p$, and $\mathbf{v}$ be the electrical potential, the number concentration of ionic species $j$, the pressure, and the fluid velocity relative to the particle, respectively, then, because the present problem is $\theta$-symmetric, the electric, the concentration, and the flow fields of the present problem can be described by [17,47]

$$\nabla^2\phi = -\frac{\rho + h(r,z)\rho_{fix}}{\varepsilon}, \tag{1}$$

$$\nabla \cdot \left[-D_j\left(\nabla n_j + \frac{z_j e}{k_B T} n_j \nabla\phi\right) + n_j \mathbf{v}\right] = 0 \tag{2}$$

$$\nabla \cdot \mathbf{v} = 0 \tag{3}$$

$$-\nabla p + \eta\nabla^2\mathbf{v} - \rho\nabla\phi - h(r,z)\gamma\mathbf{v} = 0 \tag{4}$$

Here, $\nabla^2$ and $\nabla$ are the Laplace operator and the gradient operator, respectively; $\varepsilon$, $\rho$ $(= \sum_{j=1}^{2} z_j e n_j)$, and $\rho_{fix}$ are the permittivity of the fluid phase, the space charge density of mobile ions, and the fixed charged density of the membrane layer, respectively; $D_j$ and $z_j$ are the diffusivity and the valance of ionic species $j$, respectively; $e$, $k_B$, and $T$ are the elementary charge, the Boltzmann constant, and the absolute temperature, respectively; $\eta$ is the fluid viscosity; $\gamma$ is the hydrodynamic frictional coefficient of the membrane layer per unit volume; $h(r,z) = 0$ for the region outside the particle, and $h(r,z) = 1$ for the region inside the membrane layer. Eq. (2), which implies that the mobile ions can be driven by the flow of fluid, the ionic concentration gradient, and the electric field, is a statement of the conversation of ionic species $j$. Eqs. (3) and (4) are the continuity equation and a modified Navier–Stokes equation, respectively, with $-\rho\nabla\phi$ and $-\gamma\mathbf{v}$ being respectively the electric body force acting on the fluid and the frictional force exerted on the fluid by the composing material of the porous layer [17]. Note that because the flow field in electrophoresis is in the creeping flow regime, there is no inertial term in Eq. (4). For simplicity, we assume that the values of $\varepsilon$, $D_j$, and $\eta$ inside the membrane layer are the same as those outside the particle, and $\rho_{fix}$ is independent of the position inside the membrane layer [17]. Duval et al. [48] verified experimentally that if the water content within the membrane layer is sufficiently high, then the $\varepsilon$ inside the membrane layer and that outside it can be assumed equal.

We assume that the strength of $\mathbf{E}$ is much weaker than that of the equilibrium electric field established by the particle and/or the boundary [49]. Similar to the treatments of Yeh and Hsu [47], each dependent variable is partitioned into an equilibrium term coming from the particle in the absence of $\mathbf{E}$, and a perturbed term from the application of $\mathbf{E}$. Because both the electrical potential and the thickness of double layer are arbitrary, the effect of DLP can be significant, implying that the double layer surrounding the particle can be asymmetric. Under these conditions, the equations governing the present problem can be summarized as following [47]:

$$\nabla^{*2}\phi_e^* = -\frac{(\kappa a)^2}{1+\alpha}[\exp(-\phi_e^*) - \exp(\alpha\phi_e^*)] - h(r,z)Q^* \tag{5}$$

$$\nabla^{*2}\delta\phi^* = \frac{(\kappa a)^2}{1+\alpha}[(\delta\phi^* = g_1^*)\exp(-\phi_e^*) + \alpha(\delta\phi^* + g_2^*)\exp(\alpha\phi_e^*)] \quad (6)$$

$$\nabla^{*2}g_1{}^* - \nabla^*\phi_e{}^* \cdot \nabla^* g_1{}^* = Pe_1\mathbf{v}^* \cdot \nabla^*\phi_e{}^* \quad (7)$$

$$\nabla^{*2}g_2{}^* + \alpha\nabla^*\phi_e{}^* \cdot \nabla^* g_2{}^* = Pe_2\mathbf{v}^* \cdot \nabla^*\phi_e{}^* \quad (8)$$

$$\nabla^* \cdot \mathbf{v}^* = 0 \quad (9)$$

$$-\nabla^*\delta p^* + \nabla^{*2}\mathbf{v}^* + [(\nabla^{*2}\phi_e{}^* + h(r,z)Q^*)\nabla^*\delta\phi^* + \nabla^{*2}\delta\phi^*\nabla^*\phi_e{}^*] - h(r,z)(\lambda a)^2\mathbf{v}^* = \mathbf{0} \quad (10)$$

$$n_1{}^* = \exp(-\phi_e{}^*)[1 - (\delta\phi^* + g_1{}^*)] \quad (11)$$

$$n_2{}^* = \exp(\alpha\phi_e{}^*)[1 + \alpha(\delta\phi^* + g_2{}^*)] \quad (12)$$

In these expressions, $\nabla^* = a\nabla$, $\nabla^{*2} = a^2\nabla^2$, $\phi_e^* = \phi_e/\phi_r$, $\delta\phi_e^* = \delta\phi_e/\phi_r$, $g_j^* = g_j/\phi_r$, $\alpha = -z_2/z_1$, $n_j{}^* = n_j/n_{j0}$, $\delta p^* = \delta p/[\varepsilon(\phi_r)^2/a^2]$, and $\mathbf{v}^* = \mathbf{v}/U_r$ with $\phi_r = k_BT/ez_1$ and $U_r = \varepsilon(\phi_r)^2/\eta a$. The subscript $e$ and the prefix $\delta$ denote the equilibrium and the perturbed properties, respectively [49]. $g_j$ is a hypothetical perturbed function simulating the polarized double layer; $n_{j0}$ is the bulk number concentration of ionic species $j$; $\kappa = [\sum_{j=1}^{2} n_{j0}(ez_j)^2/\varepsilon\kappa_BT]^{1/2}$ is the reciprocal Debye length; $Q^* = \rho_{fix}a^2/\varepsilon\phi_r$ is the scaled fixed charge density of the membrane layer; $Pe_j = \varepsilon(\phi_r)^2/\eta D_j$ is the electric Peclet number of ionic species $j$. $\lambda^{-1} = (\eta/\gamma)^{1/2}$ is the softness parameter of the membrane layer [20], or a shielding length characterizing the extent of flow penetration into that layer [50]. For biocolloids [18,40], $\lambda^{-1}$ ranges typically from 0.1 to 10 nm.

To simulate biocolloids [18,40], we assume that the surface of the rigid core of the particle is uncharged, nonconductive, impermeable to ionic species, and non-slip. These yield the following boundary conditions:

$$\mathbf{n} \cdot \nabla^*\phi_e^* = 0 \quad (13)$$

$$\mathbf{n} \cdot \nabla^*\delta\phi^* = 0 \quad (14)$$

$$\mathbf{n} \cdot \nabla^* g_j^* = 0, \quad j = 1, 2 \quad (15)$$

$$\mathbf{v}^* = \mathbf{0} \quad (16)$$

Here, $\mathbf{n}$ is the unit normal vector directed into the liquid phase. The boundary conditions assumed on the cavity and on the membrane layer–fluid interface are summarized in Supplementary Material.

Instead of solving the original problem directly, two hypothetical sub-problems are solved, which is capable of avoiding a tedious trial-and-error procedure arising from the unknown electrophoretic velocity in the boundary conditions [28]. In the first sub-problem the particle moves with a constant velocity $U$ in the absence of $\mathbf{E}$, and in the second sub-problem $\mathbf{E}$ is applied but the particle is held fixed. Detailed solution procedure for the scaled electrophoretic mobility of a particle, $\mu^* = (U^*/E^*)$, with $U^* = U/U_r$ and $E^* = E/(\phi_r/a)$ being respectively the dimensionless electrophoretic velocity of a particle and the dimensionless strength of $\mathbf{E}$ in the $z$ direction, is presented in Supplementary Material.

## 3. Results and discussion

The governing equations and the associated boundary conditions are solved numerically by FlexPDE (version 4.24, PDE Solutions, Spokane Valley, WA), which is based on a finite-element method. The numerical scheme and its implementation using FlexPDE have been validated to be efficient and sufficiently accurate for solving similar boundary-value problems [29–32,47,51].

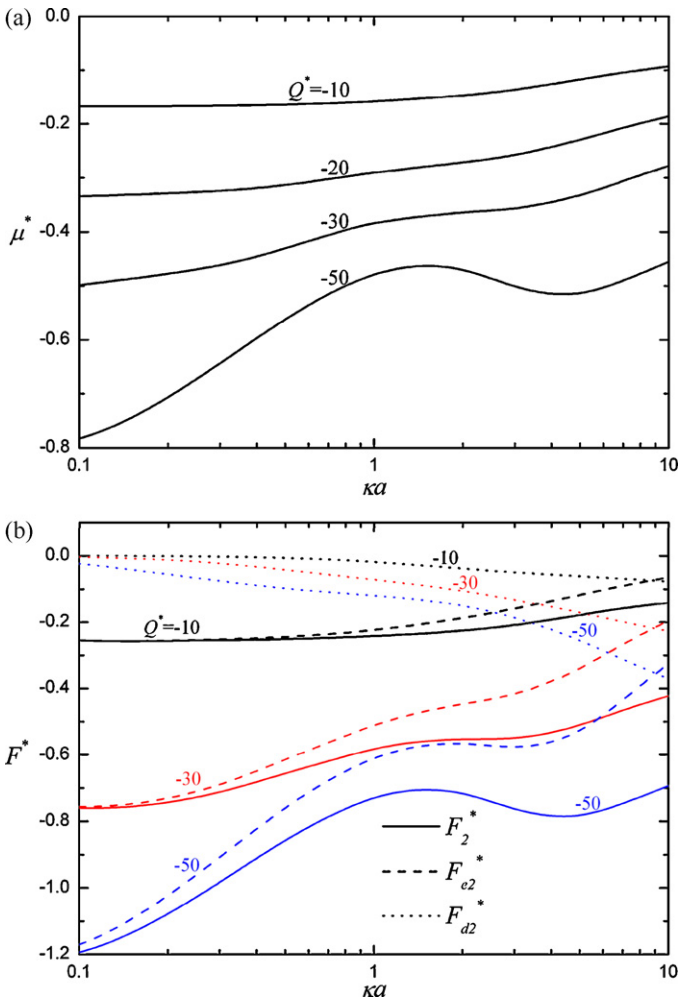


**Fig. 1.** Variations of the scaled electrophoretic mobility $\mu^*$, (a), and the corresponding scaled forces in sub-problem two, $F_{e2}^*$, $F_{d2}^*$, and $F_2^*$, (b), as a function of $\kappa a$ for various values of $\mu^*$ at $M = 0\%$, $\Lambda = 0.5$, $c/a = 0.25$, and $\lambda a = 4$.

In subsequent discussions, the influences of the key parameters of the present problem, including the thickness of double layer, the properties of the membrane layer of the particle, and the size and the position of the particle on its electrophoretic behavior are examined in detail through numerical simulation. Unless otherwise specified, we let $Pe_1 = Pe_2 = 0.1$ [47], which is usually assumed in relevant electrokinetic studies for the case where the effect of DLP can be significant. We focus on type II soft particles, that is, biocolloids.

### 3.1. Influence of double layer thickness and fixed charged density of membrane layer

Fig. 1 presents the simulated variations of the scaled electrophoretic mobility of a particle, $\mu^*$, and the corresponding scaled forces acting on the particle in the second sub-problem, $F_{e2}^*$, $F_{d2}^*$, $F_2^* = (F_{e2}^* + F_{d2}^*)$, as a function of the scaled double layer thickness, $\kappa a$, at various values of $Q^*$. Here, because we fix the radius of the particle $a$, the variation of $\kappa a$ comes from that of the bulk electrolytes concentration. As seen in Fig. 1(a), the qualitative behavior of $\mu^*$ depends largely on the level of $Q^*$. If $|Q^*|$ is small, then $|\mu^*|$ decreases monotonically with increasing $\kappa a$. However, if $|Q^*|$ is sufficiently large (e.g., $Q^* = -50$), then as $\kappa a$ varies, $|\mu^*|$ has a local minimum occurring at $\kappa a \cong 1.5$. The occurrence of the local minimum in $|\mu^*|$ can be explained by the following. At smaller values of $\kappa a$, the membrane layer of the particle is enclosed by the

double layer. In this case, an increase in $\kappa a$ (decrease in double layer thickness) yields an increase in the amount of counterions confined inside the membrane layer, leading to a decrease in the absolute value of the effective charge density, $|\rho + \rho_{fix}|$, inside that layer and, therefore, a decrease in the electrical driving force acting on the particle, as is verified by Fig. 1(b). This behavior is consistent with the typical electrophoretic behavior of microorganisms [18], biological cells [18,48], and biocolloids [39,40], but inconsistent with that of type I soft particles [31–38]. This is because a Dirichlet type of boundary condition, imposing a constant surface potential, is applied on the surface of the rigid core of the particle in the latter. Therefore, as $\kappa a$ increases, although $|\rho + \rho_{fix}|$ decreases, the charge density on that surface increases [32]. The competition between these two effects is capable of yielding complicated electrophoretic behaviors [32]. However, if $|Q^*|$ is large, then the electrical potential of the system is high, implying that the effect of DLP is significant. This effect, which is most important when the thickness of double layer is comparable to the particle size [28], usually reduces the particle mobility. Therefore, it can be inferred that the presence of the local minimum in $|\mu^*|$ at $\kappa a \cong 1.5$ is due to the effect of DLP. The presence of the local minimum in $|\mu^*|$ was also observed in the theoretical study of O'Brien and White [28] for the case of an isolated rigid sphere in an infinite fluid, that of Yeh and Hsu [47] for the case of a charged porous sphere in a cylindrical pore, that of Huang et al. [38] for the case of a membrane-coated sphere in a cylindrical pore, and in several experimental studies for the case of polyelectrolytes [52] and silica colloids [53]. The electrophoretic behaviors seen in Fig. 1(a) will be verified later by the experimental results in the literature.

The qualitative behavior of $\mu^*$ seen in Fig. 1(a) is similar to that of $F_2^*$ illustrated in Fig. 1(b), implying that the qualitative behavior of $\mu^*$ as $Q^*$ and $\kappa a$ vary depends mainly on the two competing driving forces, $F_{e2}^*$ and $F_{d2}^*$. Fig. 1(b) also suggest that in the case considered, $\mu^*$ is mainly dominated by $F_{e2}^*$. This implies that for the present type of soft, biocolloidal particle (type II soft particle), the influence of $Q^*$ on the behavior of $\mu^*$ as $\kappa a$ varies is dominated mainly by the electrical driving force coming from **E**. This is different from the case of a membrane-coated soft particle (type I soft particle) in the literature [25–27,31–38], where that behavior is dominated by the competition between the electrical driving force and the electroosmotic retardation force $F_{d2}^*$ [32]. Note that the larger the $Q^*$ the more significant the effect of DLP, making the presence of the local minimum in $\mu^*$ occurring at $\kappa a \cong 1$ more pronounced. More detailed discussion on the influence of $Q^*$ on the scaled forces acting on a particle is given in Supplementary Material.

### 3.2. Influence of softness of membrane layer

The influence of the friction coefficient (or softness) of the membrane layer of a particle, measured by $\lambda a$, on its scaled mobility $\mu^*$ is illustrated in Fig. 2; the corresponding scaled forces, $F_{e2}^*$, $F_{d2}^*$, and $F_i^* (= F_{ei}^* + F_{di}^*)$ acting on the particle are also presented. It is interesting to note that the qualitative behavior of $\mu^*$ depends highly upon the level of $\lambda a$. If $\lambda a$ is small, the influence of the effect of DLP on the electrophoretic behavior of the soft particle is significant. In this case, $|\mu^*|$ has a local minimum occurring at a $\kappa a$ in the range [1.0,2.0], which is consistent with the result shown in Fig. 1. On the other hand, if $\lambda a$ is large, then that effect becomes insignificant. In this case, $|\mu^*|$ is seen to decreases with increasing $\kappa a$, which is unexpected. These behaviors can be explained by the variations of $F_{e2}^*$ and $F_{d2}^*$ shown in Fig. 2(b). This figure indicates that $F_{e2}^*$ is uncorrelated with $\lambda a$, and $|F_{e2}^*|$ decreases with increasing $\kappa a$. In addition, if $\lambda a$ is small, then $F_{d2}^*$ is negative and $|F_{d2}^*|$ increases monotonically with increasing $\kappa a$. On the other hand, if $\lambda a$ is sufficiently large, then $F_{d2}^*$ is negative at small values of $\kappa a$, passing through a

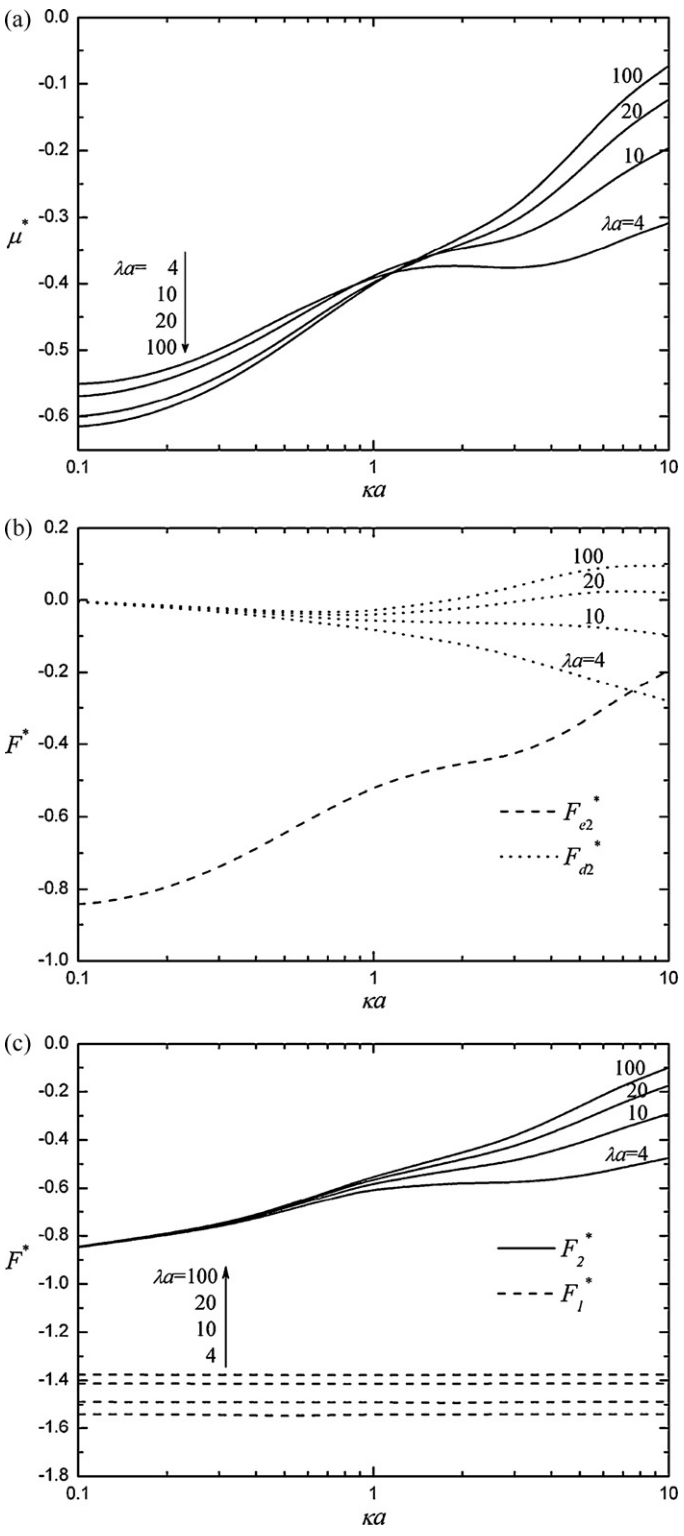


**Fig. 2.** Variations of the scaled electrophoretic mobility $\mu^*$, (a), and the corresponding scaled forces, $F_{e2}^*$ and $F_{d2}^*$, (b), and $F_1^*$ and $F_2^*$, (c), as a function of $\kappa a$ for various values of $\lambda a$ at $M = 0\%$, $\Lambda = 0.5$, $c/a = 0.3$, and $Q^* = -30$.

negative local minimum near $\kappa a \cong 1$, and then becomes positive if $\kappa a$ is sufficiently large. These imply that, if $\lambda a$ is small, the electroosmotic retardation flow arising from the motion of the counterions in the double layer due to **E** enhances the effect of DLP. On the other hand, if $\lambda a$ is large, that flow offsets the effect of DLP, making the local minimum of $|\mu^*|$ at $\kappa a \cong 1$ disappears. That $F_{d2}^*$ can be

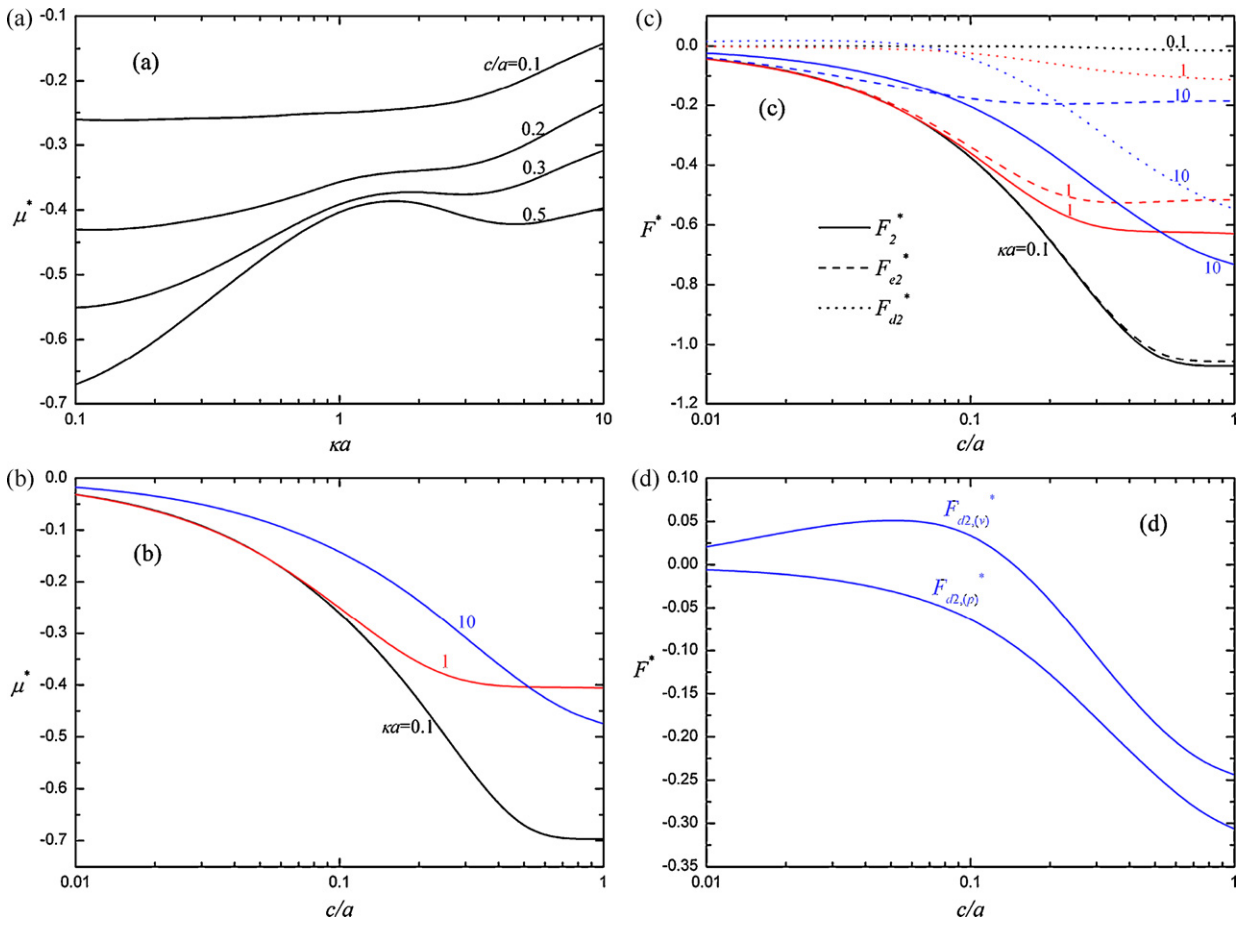


**Fig. 3.** Variations of the scaled electrophoretic mobility $\mu^*$ as a function of $\kappa a$ for various values of $(c/a)$, (a), that as a function of $(c/a)$ for various values of $\kappa a$, (b), at $M = 0\%$, $\Lambda = 0.5$, $\lambda a = 4$, and $Q^* = -30$; variations of the corresponding scaled forces in sub-problem two, $F^*_{e2}$, $F^*_{d2}$, and $F^*_2$, for the case of (b), (c), and that of $F^*_{d2,(p)}$ and $F^*_{d2,(v)}$ for the case of (c) at $\kappa a = 10$, (d).

positive seen in Fig. 2(b) is also observed in the electrophoresis of a negatively charged, rigid sphere towards a large disk [54]. In this case, the rate of strain across the particle surface is positive, and increases with increasing $\kappa a$, so is the viscous component of $F^*_{d2}$, $F^*_{d2,(v)}$. Therefore, if $\kappa a$ is sufficiently large, then although the pressure component of $F^*_{d2}$, $F^*_{d2,(p)}$, is always negative, $F^*_{d2,(v)}$ becomes positive and dominates the behavior of $F^*_{d2}$. Fig. 2(a) also reveals that if $\kappa a$ is large, then $|\mu^*|$ decreases with increasing $\lambda a$, but the reverse trend is observed if $\kappa a$ is small. The former is also observed in the other similar electrophoresis problems [31–38], where type I soft particle is simulated, and can be explained by that the larger the $\lambda a$ the greater the friction force coming from the membrane layer. The later has not been reported previously, and can be explained by the competition between $F^*_1$ and $F^*_2$ as $\lambda a$ varies, shown in Fig. 2(c). As seen in this figure, if $\kappa a$ is small, then the rate of decrease in $|F_1{}^*|$ with increasing $\lambda a$ is always faster than that in $|F_2{}^*|$, yielding a monotonic increase in $|\mu^*|$ with increasing $\lambda a$. We conclude that the softness of the membrane layer of the present type of soft particle is capable of influencing both quantitatively and qualitatively its electrophoretic behavior.

### 3.3. Influence of the thickness of membrane layer

The influence of the thickness of the membrane layer of a particle on its electrophoretic behavior is illustrated in Fig. 3(a) and (b), and the corresponding variations of the scaled forces, $F^*_{e2}$, $F^*_{d2}$, and $F^*_2$ for the case of Fig. 3(b) are presented in Fig. 3(c). As seen in Fig. 3(a), the qualitative behavior of $\mu^*$ as $\kappa a$ varies depends highly upon the scaled membrane thickness $(c/a)$. If $(c/a)$ is small, then $|\mu^*|$ decreases monotonically with increasing $\kappa a$. On the other hand, if $(c/a)$ is large, then $|\mu^*|$ has a local minimum occurring at $\kappa a \cong 1.7$. Again, these behaviors arise from the competition between the electrical driving force and the electroosmotic retardation force. For the present case, because the volume of the membrane layer of the particle increases with increasing $(c/a)$, so are the amount of fixed charge and the associated electrical driving force. Therefore, the larger the $(c/a)$ the higher the electrical potential, the more significant the effect of DLP and, therefore, the more apparent the presence of the local minimum in $\kappa a$. Fig. 3(b) shows the variations of $\mu^*$ as a function of $(c/a)$ at varies values of $\kappa a$. Note that if $\kappa a$ is large, then $|\mu^*|$ increases monotonically with increasing $(c/a)$. On the other hand, if it is small, $|\mu^*|$ increases with increasing $(c/a)$ first, and then approaches a constant value as $(c/a)$ gets large. Fig. 3(b) and (c) reveals that the qualitative behaviors of $\mu^*$ are similar to those of $F^*_2$, implying that the behaviors of $\mu^*$ as $\kappa a$ and $(c/a)$ vary depend upon the result of the competition between $F^*_{e2}$ and $F^*_{d2}$. If $\kappa a$ is sufficiently small (double layer is sufficiently thick), then the behavior of $\mu^*$ as $(c/a)$ varies is dominated by $F^*_{e2}$. On the other hand, if $\kappa a$ is sufficiently large (double layer is sufficiently thin), then that behavior is dominated by $F^*_{e2}$ when $(c/a)$ is small, and by $F^*_{d2}$ when $(c/a)$ is large. If $\kappa a$ takes a medium large value (=1), then the behavior of $\mu^*$ is dominated by $F^*_{e2}$ when $(c/a)$ is small, and by both $F^*_{e2}$ and $F^*_{d2}$ when $(c/a)$ is large. As mentioned previously, these behaviors result from that although $|F^*_{e2}|$ is larger at a smaller $\kappa a$, the influence of the electroosmotic retardation flow becomes significant when $\kappa a$ is sufficiently large, yielding a stronger $|F^*_{d2}|$. In addition, if the membrane layer of a particle is sufficiently thick, because the amount

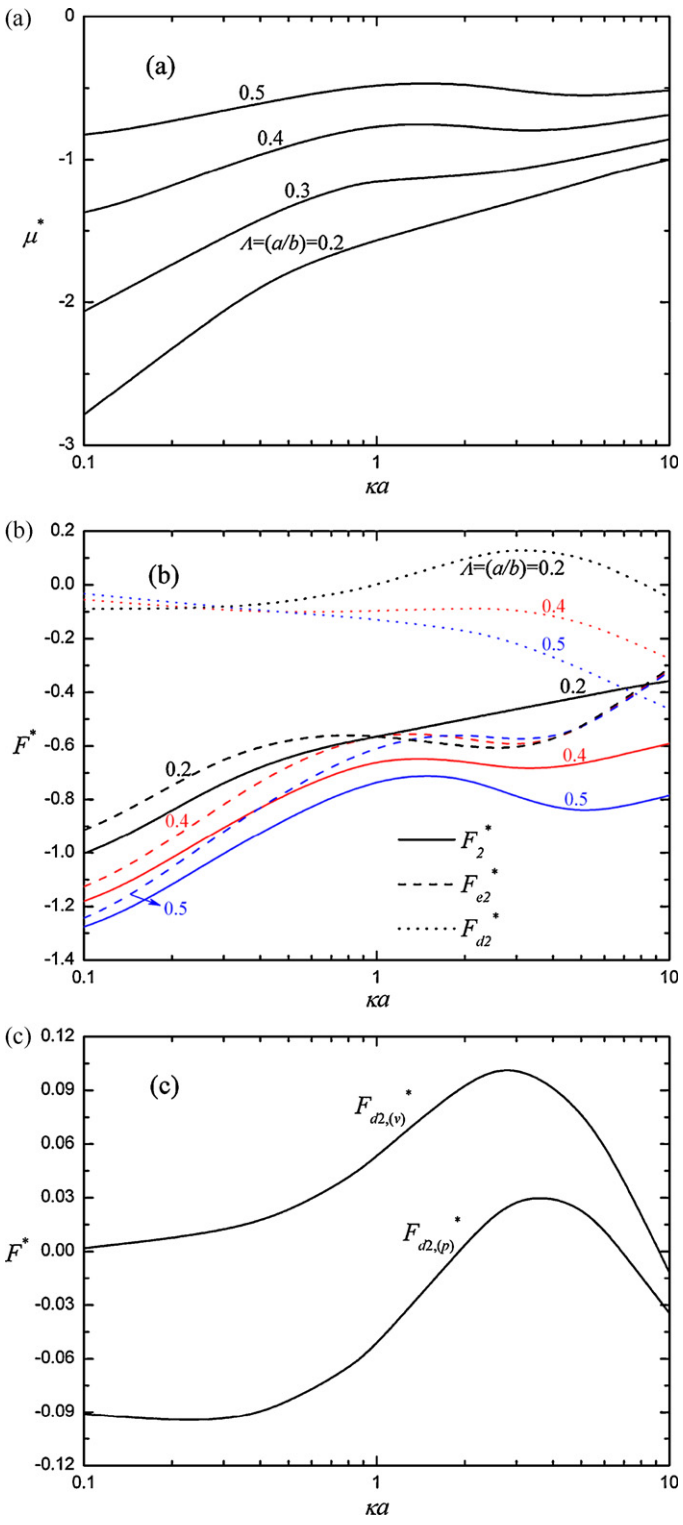


**Fig. 4.** Variations of the scaled electrophoretic mobility $\mu^*$ as a function of $\kappa a$ for various values of $\Lambda$, (a), at $M = 0\%$, $c/a = 0.3$, $\lambda a = 4$, and $Q^* = -50$; variations of the corresponding scaled forces in sub-problem two, $F^*_{e2}$, $F^*_{d2}$, and $F^*_2$, for the case of (a), (b), and that of $F^*_{d2,(p)}$ and $F^*_{d2,(v)}$ for the case of (b) at $\Lambda = 0.2$, (c).

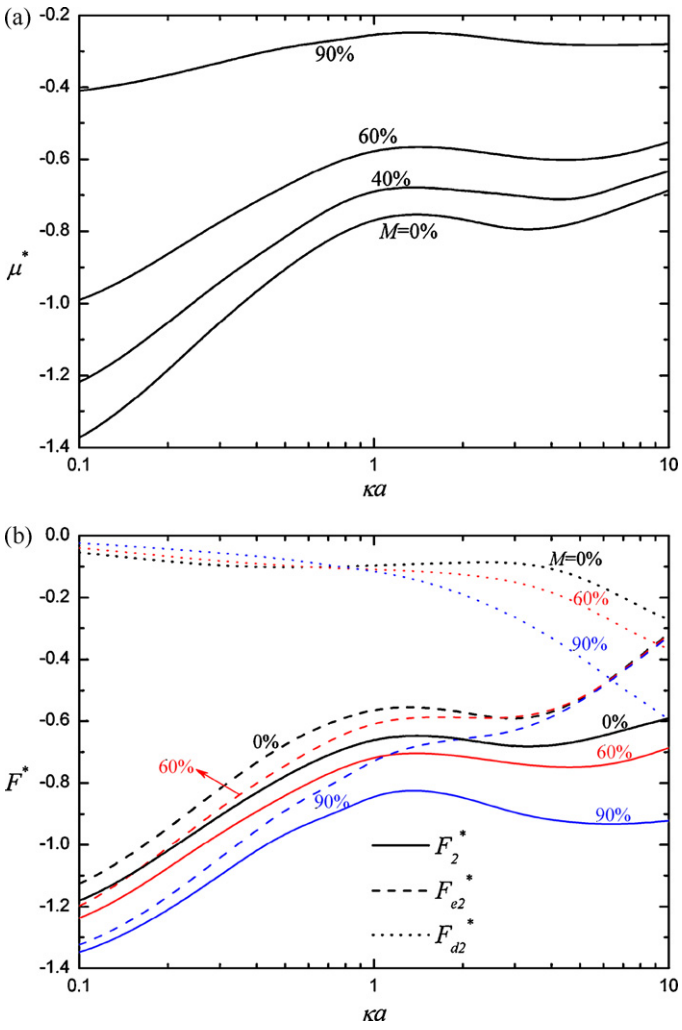


**Fig. 5.** Variations of the scaled electrophoretic mobility $\mu^*$, (a), and the corresponding scaled forces in sub-problem two, $F^*_{e2}$, $F^*_{d2}$, and $F^*_2$, (b), as a function of $\kappa a$ for various values of $M$ at $\Lambda = 0.4$, $c/a = 0.3$, $\lambda a = 4$, and $Q^* = -50$.

of fixed charge in that layer increases with increasing membrane thickness, so is the significance of the effect of DLP, thereby reducing the electrical driving force and making $\mu^*$ roughly constant as $(c/a)$ varies, as seen in Fig. 3(b). This can be verified by the behavior of $F^*_{e2}$ shown in Fig. 3(c), where $|F^*_{e2}|$ increases with increasing $(c/a)$, and shows a local maximum at a large $(c/a)$. The former arises from that the thicker the membrane layer the more the amount of fixed charge it carries and, therefore, the greater the electrical driving force. It is interesting to see in Fig. 3(c) that at $\kappa a = 10$, the increasing of $|F^*_{e2}|$ with increasing $(c/a)$ is more apparent for $(c/a) < (1/\kappa a) = 0.1$ than that for $(c/a) < (1/\kappa a) = 0.1$. This is because if the double layer is sufficiently thick, then its overlapping with the membrane layer of the particle is significant, and the variation of $|F^*_{e2}|$ with $(c/a)$ is influenced accordingly. Fig. 3(c) also reveals that if $\kappa a$ is small, $F^*_{d2}$ is negative and $|F^*_{d2}|$ increases with increasing $(c/a)$. On the other hand, if $\kappa a$ is sufficiently large (ca. 10), then $F^*_{d2}$ may change its sign from positive to negative as $(c/a)$ increases, and $|F^*_{d2}|$ increases with increasing $(c/a)$ if $(c/a)$ is sufficiently large. Similar to the cases of Figs. 1(b) and 2(b), these behaviors arise mainly from the competition between $F^*_{d2,(v)}$ and $F^*_{d2,(p)}$, as illustrated in Fig. 3(d). More detailed discussion is presented in Supplementary Material.

### 3.4. Influence of the boundary

The influence of a boundary on the electrophoretic behavior of a soft particle is illustrated in Figs. 4–6. Here, the boundary effect is measured by the relative cavity size $\Lambda$ $(=a/b)$ and the position parameter $M = 100\% \times [m/(b-a)]$. Fig. 4 shows the variations of the scaled mobility $\mu^*$ as a function of $\kappa a$ at various values of $\Lambda$; the corresponding scaled forces in the second sub-problem, $F^*_{e2}$, $F^*_{d2}$, $F^*_2$,

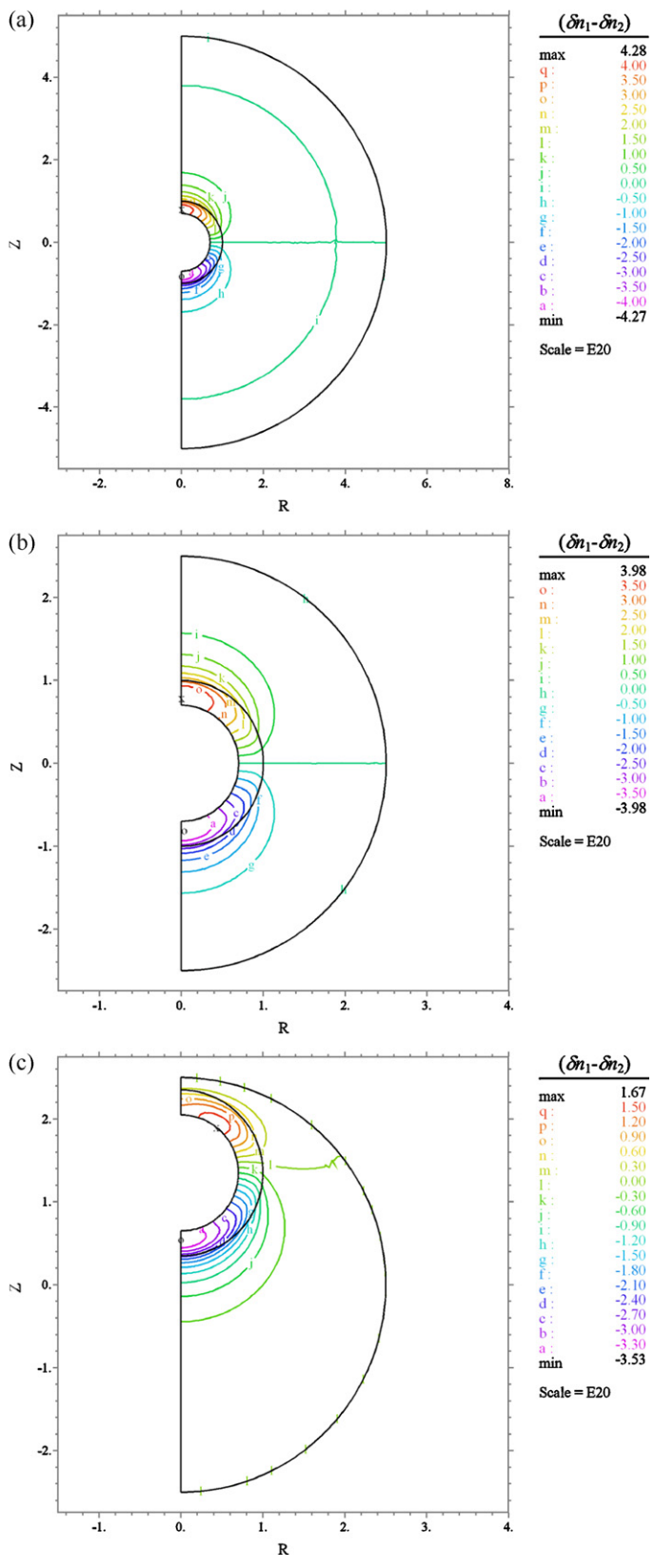


**Fig. 6.** Contours of the net perturbed ionic concentration difference $(\delta n_1 - \delta n_2)$ in sub-problem two on the half plane $\theta = 0$ for the cases of Figs. 4(a) and 5(a) at $\kappa a = 1$. (a) $\Lambda = 0.2$ and $M = 0\%$; (b) $\Lambda = 0.4$ and $M = 0\%$; (c) $\Lambda = 0.4$ and $M = 90\%$.

$F^*_{d2,(v)}$, and $F^*_{d2,(p)}$, at several selected values of $\Lambda$ and $\kappa a$ are also presented. It is interesting to note that the qualitative behavior of $\mu^*$ as $\kappa a$ varies depends largely upon the level of $\Lambda$. As seen in Fig. 4(a), if $\Lambda$ is large, although DLP is influenced significantly by the boundary, the influence of the effect of DLP on the behavior of $\mu^*$ is pronounced due to the effect of electroosmotic retardation flow. In this case, $|\mu^*|$ decreases with increasing $\kappa a$ and has an local minimum occurring at $\kappa a \cong 1$, which is similar to the case of Fig. 1(a) at $Q^* = -50$. On the other hand, if $\Lambda$ is small, although DLP is uninfluenced by the boundary, its influence on $\mu^*$ is inappreciable due to the effect of electroosmotic retardation flow, the local minimum in $|\mu^*|$ disappears. In this case, $|\mu^*|$ decreases monotonically with increasing $\kappa a$, which is qualitatively consistent with many experimental results reported in the literature [18,20,39,40,48]. Again, these behaviors arise from the competition of $F^*_{e2}$ and $F^*_{d2}$, as $\Lambda$ and $\kappa a$ vary. As seen in Fig. 4(b), the behaviors of $F^*_{e2}$ at various values of $\Lambda$ are similar, namely, $|F^*_{e2}|$ decreases with increasing $\kappa a$ and has a local minimum occurring at a medium large $\kappa a$ due to the effect of DLP, which is consistent with the result shown in Fig. 1(b), and can be explained by the same reasoning. Also in Fig. 4(b), because the larger the $\Lambda$ the more significant the boundary effect and, therefore, the less appreciable the presence of the local minimum in $|F^*_{e2}|$. This is because if $\Lambda$ is large, then the double layer surrounding the particle is compressed significantly by the boundary. In this case, if $\kappa a$ is small, then coions are pushed into the membrane layer of the particle, which has the effect of raising $|F^*_{e2}|$, and $|F^*_{e2}|$ increases with increasing $\Lambda$. In addition, if $\Lambda$ is large, the flow field surrounding the particle is also compressed by the boundary, which has the effect of alleviating the effect of DLP, as will be verified later. These two effects lead to the behaviors of $|F^*_{e2}|$ as $\Lambda$ and $\kappa a$ vary seen in Fig. 4(b). This figure also indicates that if $\Lambda$ is large, then $F^*_{d2}$ is negative and $|F^*_{d2}|$ increases with increasing $\kappa a$, which is consistent with the results shown in Fig. 1(b), and can be explained by the same reasoning as that employed in the discussion of Fig. 1(b). On the other hand, if $\Lambda$ is small, then $F^*_{d2}$ is negative at small $\kappa a$ and $|F^*_{d2}|$ decreases with increasing $\kappa a$, but if $\kappa a$ is sufficiently large, then $F^*_{d2}$ might change its sign from negative to positive and has a positive local maximum as $\kappa a$ varies. As seen in Fig. 4(b), the presence of a positive local maximum in $F^*_{d2}$ makes it possible that $F^*_{d2}$ changes its sign twice as $\kappa a$ varies. As illustrated in Fig. 4(c), these behaviors at a small value of $\Lambda$ arise from the competition between $F^*_{d2,(v)}$ and $F^*_{d2,(p)}$, and the behaviors of them depend upon the electroosmotic retardation flow surrounding the particle. More detail discussion is presented in Supplementary Material. Therefore, if the boundary effect is significant (large $\Lambda$), then because the electrophoretic behavior of a particle is dominated by the electrical driving force, the influence of the effect of DLP on the behavior of $\mu^*$ is enhanced, although the larger the $\Lambda$ the less significant that effect is. On the other hand, if the boundary effect is insignificant (small $\Lambda$), then the electrophoretic behavior of a soft particle depends upon both the electrical driving force and the hydrodynamic force coming from the electroosmotic retardation flow. This implies that the former influence can be offset by the latter one, and therefore, $|\mu^*|$ decreases with increasing $\kappa a$.

Fig. 5(a) shows the variations of $\mu^*$ as a function of $\kappa a$ at various values of $M$, and the corresponding variations of the scaled forces in the second sub-problem, $F^*_{e2}$, $F^*_{d2}$, $F^*_2$, are presented in Fig. 5(b). As seen in Fig. 5(a), $|\mu^*|$ has a local minimum for $\kappa a$ in the range [1.0,2.0], which is consistent with the result shown in Fig. 1(a), and can be explained by the similar reasoning. It is interesting to note that the larger the $M$ the less appreciable the presence of that local minimum in $|\mu^*|$. Similar to the reasoning employed in the discussion of Fig. 4, this phenomenon arises from that as $M$ increases, the effect of DLP is alleviated by the depression of the flow field surrounding the particle by the boundary and by the increase in the

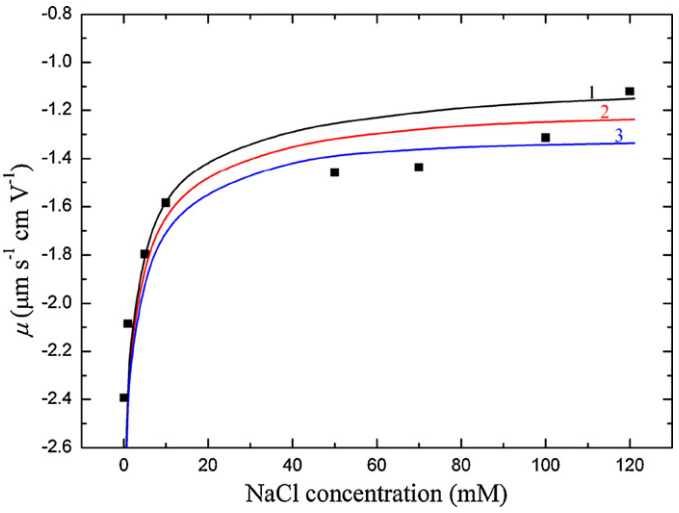


**Fig. 7.** Variation of the electrophoretic mobility of creatine-covered gold nanoparticles $\mu$ (=$U/E$) as a function of NaCl concentration for the case where the soft nanoparticles of radius 15 nm comprises a rigid gold core of radius 10.5 nm and an ion-penetrable membrane layer of thickness 4.5 nm. Discrete symbols: experimental data of López-Viota et al. [40]; curves: results based on this study. Curve 1, $\rho_{fix}/F = -25$ mol/m$^3$ and $\lambda^{-1} = 3.33$ nm, 2, $\rho_{fix}/F = -25$ mol/m$^3$ and $\lambda^{-1} = 3.75$ nm, 3, $\rho_{fix}/F = -25$ mol/m$^3$ and $\lambda^{-1} = 4.29$ nm. Other parameters used are $M = 0\%$, $D_1 = 1.33 \times 10^{-9}$ m$^2$/s, $D_2 = 2.03 \times 10^{-9}$ m$^2$/s, $Pe_1 = 0.351$, $Pe_2 = 0.23$, and $\Lambda = 0.08$.

amount of coions inside the membrane layer of the particle due to the overlapping of the double layer surrounding the particle and the cavity, and $|F^*_{e2}|$ increases accordingly, as seen in Fig. 5(b). This figure also reveals that if $M$ is small, then because the DLP effect is significant $F^*_2$ is dominated by $F^*_{e2}$. On the other hand, if $M$ is large, then because that effect is insignificant, both $F^*_{e2}$ and $F^*_{d2}$ can contribute comparably to $F^*_2$. The dependence of the effect of DLP on $\Lambda$ and $M$ can be illustrated by the contours of the net perturbed ionic concentration difference, $(\delta n_1 - \delta n_2)$, shown in Fig. 6. This figure shows that the larger the $\Lambda$ and/or $M$, because the more significant the boundary effect is, the less significant the effect of DLP. It should be pointed out that this is the first attempt in the literature to show the evidence for the influence of a boundary on the effect of DLP and on the electrophoretic behavior of type II soft particles.

### 3.5. Verification with experimental data

In this section, the applicability of our model in fitting experimental results is examined. For illustration, it is adopted to describe the experimental data of López-Viota et al. [40], where the electrophoresis of creatine-covered gold nanoparticles of radius 15 nm, comprising a rigid gold core of radius 10.5 nm and an ion-penetrable membrane layer of thickness 4.5 nm [40], in an aqueous NaCl solution was conducted. The relevant physical constants are $z_1 = -z_2 = 1$, $\varepsilon = 7.08 \times 10^{-10}$ CV$^{-1}$ m$^{-1}$, $k_B = 1.38 \times 10^{-23}$ J/K, $T = 298$ K, $\eta = 10^{-3}$ kg m$^{-1}$ s$^{-1}$, $e = 1.6 \times 10^{-19}$ C, $D_1 = 1.33 \times 10^{-9}$ m$^2$ s$^{-1}$, and $D_2 = 2.03 \times 10^{-9}$ m$^2$ s$^{-1}$. To avoid the influence of the boundary, $\Lambda$ (=$a/b$) is assumed a small value of 0.08 [51]. Fig. 7 shows the variation of the electrophoretic mobility $\mu$ as a function of the concentration of NaCl. Both the experimental data [40] and the results predicted by the present theoretical model are presented. The latter are based on three sets of parameter values, namely, ($\rho_{fix}/F = -25$ mol/m$^3$, $\lambda^{-1} = 3.33$ nm), ($\rho_{fix}/F = -25$ mol/m$^3$, $\lambda^{-1} = 3.75$ nm), and ($\rho_{fix}/F = -25$ mol/m$^3$, $\lambda^{-1} = 4.29$ nm), where $F$ is Faraday constant. These lead to ($Q^* = -29.84$, $\lambda a = 4.5$), ($Q^* = -29.84$, $\lambda a = 4$), and ($Q^* = -29.84$, $\lambda a = 3.5$), respectively. As seen in Fig. 7, the present theoretical model predicts successfully the general trend of the mobility of the particle. The estimated values of $(\rho_{fix}/F)$ and $\lambda^{-1}$ are different from those estimated by another three simplified theoretical models, where the effect of double-layer polarization arising from the convective motion of ionic species is neglected, used by López-Viota et al. [40] Note that at the present level of charge density, $Q^* = -29.84$, that effect is expected to be significant. Fig. 7 also reveals that as the concentration of NaCl gets high, the mobility approaches a non-zero constant value, which is typical to soft biocolloids (type II soft particle) [17,18]. In contrast, the mobility of rigid particles with constant surface charge density approaches zero as the concentration of electrolyte gets high. As seen in Figs. 1–5, if the fixed charge density of the membrane layer of a particle is sufficiently high, then the effect of DLP on its electrophoretic behavior becomes significant. This yields an extra local minimum in its mobility, which occurs at a moderate high electrolyte concentration (i.e., medium large $\kappa a$). Similar behavior was also observed in the experimental results presented in Figs. S6 and S7 of Supplementary Material (the curve corresponds to 15 nm gold nanoparticles in Fig. S6 [55], and the curves correspond to temperature lower than 32.5 °C in Fig. S7 [56]), but the rationale behind that behavior was not explained explicitly. The present analysis is capable of providing a sound interpretation of the general electrophoretic behaviors of soft biocolloids that is essential to the design of an electrophoresis device.

## 4. Conclusions

The electrophoretic behavior of a soft particle under the conditions where the effects of boundary and double-layer polarization (DLP) can be significant is investigated. We classify the soft particles in the literature into two types: type I soft particles have a charged rigid core with constant surface potential and an ion-penetrable porous layer, and type II soft particles have an uncharged rigid core and a polyelectrolyte membrane layer. We show that the electrophoretic behaviors of these two types of soft particle are different qualitatively. In particular, the mobility of a type I soft particle increases with increasing bulk ionic concentration (i.e., decreasing double layer thickness), but that trend is reversed in the case of a type II soft particle. This study provides a possible explanation for the experimentally observed behaviors of both inorganic particles covered by an artificial membrane layer (type I), such as metal oxide particles enclosed by surfactant molecules, and biocolloids such as proteins, microorganisms, and inorganic particles covered by a biological membrane layer (type II). The applicability of the present model is verified by fitting it to the experimental data of creatine-covered gold nanoparticles reported in the literature. The results of numerical simulation reveal that the interactions among boundary, DLP, and electroosmotic retardation flow yield profound electrophoretic behaviors. For the case of type II soft particles, the influences of the key parameters of the system under consideration on the electrophoretic behaviors of a soft particle can be summarized as following. (i) The qualitative behavior of the mobility of a particle as the thickness of double layer varies depends largely upon both the properties of its membrane layer and how significant the boundary effect is. (ii) If the fixed charge density of the membrane layer is low and/or the membrane layer is thin, then the absolute value of the mobility decreases with decreasing double layer thickness. On the other hand, if it is high and/or the membrane layer is thick, then the absolute value of the mobility also has a local minimum, which arises from the effect of DLP. These behaviors are consistent with the experimental observations in the literature. (iii) The significance of the effect of DLP decreases with increasing significance of the boundary effect. However, if the boundary is small and/or the friction coefficient of the membrane layer is sufficiently small, then the significance of that effect on the electrophoretic behavior of a particle is enhanced by the electroosmotic retardation

flow, yielding a local minimum in the absolute value of the mobility. On the other hand, if the boundary is large and/or the friction coefficient is large, then the effect of DLP on the behavior of a particle might be offset by the electroosmotic retardation flow, yielding the result that the mobility decreases with decreasing double layer thickness. These explain that why most of the experimental capillary electrophoresis results in the literature for biocolloids show that the mobility decreases with decreasing double layer thickness. Note that the ratio, $\kappa a$ = (linear size of particle)/(double layer thickness), in many electrophoresis experiments of biocolloids is usually large and/or the boundary effect is neglected so that the effect of DLP becomes unimportant. Unless the boundary effect is sufficiently significant and/or the friction coefficient of the membrane layer is sufficiently small, the influence of the effect of DLP on the electrophoretic behavior of soft biocolloids (type II) becomes apparent due to electroosmotic retardation flow. (iv) If the double layer is thin, then the absolute value of the mobility of a particle decreases with increasing friction coefficient of its membrane layer. However, if the double layer is sufficiently thick, then the opposite trend is observed, an interesting result which has not been found previously. These imply that, depending upon the thickness of double layer, the friction of the membrane layer can either retard or accelerate the movement of a soft particle.

## Acknowledgment

This work is supported by the National Science Council of the Republic of China.

## Appendix A. Supplementary data

Supplementary data associated with this article can be found, in the online version, at doi:10.1016/j.colsurfb.2011.07.033.

## References

[1] N.W. Frost, M. Jing, M.T. Bowser, Anal. Chem. 82 (2010) 4682.
[2] U. Pyell, Electrophoresis 31 (2010) 814.
[3] S. Haeberle, R. Zengerle, Lab Chip 7 (2007) 1094.
[4] R.B. Schoch, J.Y. Han, P. Renaud, Rev. Mod. Phys. 80 (2008) 839.
[5] P. Nandi, S.M. Lunte, Anal. Chim. Acta 651 (2009) 1.
[6] C. Dekker, Nat. Nanotechnol. 2 (2007) 209.
[7] S. Howorka, Z. Siwy, Chem. Soc. Rev. 38 (2009) 2360.
[8] S. van Dorp, U.F. Keyser, N.H. Dekker, C. Dekker, S.G. Lemay, Nat. Phys. 5 (2009) 347.
[9] H.J. Keh, S.B. Chen, J. Fluid Mech. 194 (1988) 377.
[10] H. Liu, H. Bau, H. Hu, Langmuir 20 (2004) 2628.
[11] L.H. Yeh, J.P. Hsu, Micofluid. Nanofluid. 7 (2009) 383.
[12] J.P. Hsu, L.H. Yeh, Langmuir 23 (2007) 8637.
[13] J.P. Hsu, L.H. Yeh, S.J. Yeh, J. Phys. Chem. B 111 (2007) 12351.
[14] E. Donath, V. Pastuschenko, Bioelectrochem. Bioenerg. 6 (1979) 543.
[15] S. Levine, M. Levine, K.A. Sharp, D.E. Brooks, Biophys. J. 42 (1983) 127.
[16] H. Ohshima, T. Kondo, Biophys. Chem. 39 (1991) 191.
[17] H. Ohshima, Adv. Colloid Interface Sci. 62 (1995) 189.
[18] J.F.L. Duval, F. Gaboriaud, Curr. Opin. Colloid Interface Sci. 15 (2010) 184.
[19] A.Y. Grosberg, T.T. Nguyen, B.I. Shklovskii, Rev. Mod. Phys. 74 (2002) 329.
[20] J.F.L. Duval, K.J. Wilkinson, H.P. van Leeuwen, J. Buffle, Environ. Sci. Technol. 39 (2005) 6435.
[21] H. Ohshima, J. Colloid Interface Sci. 163 (1994) 474.
[22] H. Ohshima, J. Colloid Interface Sci. 228 (2000) 190.
[23] H. Ohshima, J. Colloid Interface Sci. 269 (2004) 255.
[24] H. Ohshima, Electrophoresis 27 (2006) 526.
[25] H. Ohshima, Electrophoresis 23 (2002) 1995.
[26] H. Ohshima, J. Colloid Interface Sci. 252 (2002) 119.
[27] H. Ohshima, Colloid Polym. Sci. 283 (2005) 819.
[28] R.W. O'Brien, L.R. White, J. Chem. Soc. Faraday Trans. 2 (74) (1978) 1607.
[29] X. Zhang, J.P. Hsu, Z.S. Chen, L.H. Yeh, M.H. Ku, S. Tseng, J. Phys. Chem. B 114 (2010) 1621.
[30] J.P. Hsu, C.C. Kuo, Chem. Eng. Sci. 64 (2009) 5247.
[31] J.P. Hsu, Z.S. Chen, S. Tseng, J. Phys. Chem. B 113 (2009) 7701.
[32] L.H. Yeh, J.P. Hsu, S. Tseng, J. Phys. Chem. C 114 (2010) 16576.
[33] D.A. Saville, J. Colloid Interface Sci. 222 (2000) 137.
[34] R.J. Hill, D.A. Saville, W.B. Russel, J. Colloid Interface Sci. 258 (2003) 56.
[35] E. Lee, K.T. Chou, J.P. Hsu, J. Colloid Interface Sci. 280 (2004) 518.
[36] E. Lee, Y.P. Tang, J.P. Hsu, Langmuir 20 (2004) 9415.
[37] W.L. Cheng, Y.Y. He, E. Lee, J. Colloid Interface Sci. 335 (2009) 130.
[38] C.H. Huang, W.L. Cheng, Y.Y. He, E. Lee, J. Phys. Chem. B 114 (2010) 10114.
[39] A.J. de Kerchove, M. Elimelech, Langmuir 21 (2005) 6462.
[40] J. López-Viota, S. Mandal, A.V. Delgado, J.L. Toca-Herrera, M. Möller, F. Zanuttin, M. Balestrino, S. Krol, J. Colloid Interface Sci. 332 (2009) 215.
[41] A.L. Zydney, J. Colloid Interface Sci. 169 (1995) 476.
[42] S. Levine, G.H. Neale, J. Colloid Interface Sci. 47 (1974) 520.
[43] H. Ohshima, J. Colloid Interface Sci. 188 (1997) 481.
[44] E. Lee, C.B. Yen, J.P. Hsu, J. Phys. Chem. B 104 (2000) 6815.
[45] M. Firnkes, D. Pedone, J. Knezevic, M. Döblinger, U. Rant, Nano Lett. 10 (2010) 2162.
[46] L. Movileanu, Trends Biotechnol. 27 (2009) 333.
[47] L.H. Yeh, J.P. Hsu, Soft Matter 7 (2011) 396.
[48] J.F.L. Duval, H.J. Busscher, B. van de Belt-Gritter, H.C. van der Mei, W. Norde, Langmuir 21 (2005) 11268.
[49] J.P. Hsu, L.H. Yeh, M.H. Ku, J. Colloid Interface Sci. 305 (2007) 324.
[50] M. Zembala, Adv. Colloid Interface Sci. 112 (2004) 59.
[51] J.P. Hsu, Y.H. Tai, Langmuir 26 (2010) 16857.
[52] M. Nagasawa, A. Soda, I. Kagawa, J. Polym. Sci. 31 (1958) 439.
[53] J. Škvarla, Langmuir 23 (2007) 5305.
[54] J.P. Hsu, M.H. Ku, C.C. Kuo, Langmuir 21 (2005) 7588.
[55] S.M. Agnihotri, H. Ohshima, H. Terada, K. Tomoda, K. Makino, Langmuir 25 (2009) 4804.
[56] T. López-León, J.L. Ortega-Vinuesa, D. Bastos-González, A. Elaïssari, J. Phys. Chem. B 110 (2006) 4629.